Mesoporous Materials

DOI: 10.1002/anie.201306775

Enhancement of Chemical Stability and Crystallinity in Porphyrin-Containing Covalent Organic Frameworks by Intramolecular Hydrogen Bonds**

*Sharath Kandambeth, Digambar Balaji Shinde, Manas K. Panda, Binit Lukose, Thomas Heine, and Rahul Banerjee**

Covalent organic frameworks (COFs)[1] are a new class of porous materials that follow the same rules of reticular chemistry[2] as metal-organic frameworks (MOFs).[3] COFs can be synthesized under relatively mild conditions, using reversible condensation reactions such as boronic acid trimerization, boronate ester formation, the trimerization of nitriles, and the Schiff base reaction.[4] The reversibility of the reactions allows the structural units to self-assemble until they achieve long-range periodicity, which results in the crystallization of COFs. These frameworks exhibit an exceptional high surface area and uniform pore size distributions, and hence can be considered as promising materials for the storage of gases, separation of gas mixtures, catalysis, and charge carrier transport.[5] In general, two classes of porous COFs have been reported: a) chemically stable amorphous porous polymeric structures, often called PAFs/POPs/CTFs[6] with intrinsic porosity and b) porous COFs with high crystallinity but moderate or poor chemical stability. COFs derived from B–O, C=N bond formation reactions exhibit low chemical stability because of the reversibility of the reactions, which leads to decomposition upon exposure to water vapor and limits their effective usage in gas storage under practical conditions. Researchers have attempted to rectify these limitations by the alkylation of the COF pore walls or by pyridine doping.[7] However, these modifications were found to always lead to the decrease in the gas adsorption properties even though it enhanced the hydrolytic stability to a moderate extent. Recently, we have successfully overcome this problem by introducing -OH functionalities adjacent to the Schiff base centers in COFs by using a methodology of combined reversible and irreversible organic reactions.[8] The expected enol-imine (-OH) form undergoes irreversible proton tautomerism to the keto-enamine form, which is stable and remains crystalline in acid (9 N HCl), base (9 N NaOH), and water.

Since 2D porphyrin-containing COFs have been reported to show high-rate charge carrier conduction and photoconductivity because of the long-range π-orbital overlapping of porphyrin units,[5a,d,9] we decided to use this keto-enamine COF formation reaction strategy to synthesize chemically stable and crystalline porphyrin-containing COFs. However, it was quite obvious that this keto-enamine COF formation strategy to synthesize porphyrin-containing COFs by the reaction of 5,10,15,20-tetrakis(4-aminophenyl)-21*H*,23*H*-porphine (C_4 symmetry) with 1,3,5-triformyl phloroglucinol (C_3 symmetry) would result in the formation of a 3D architecture.[4a] Moreover since the proton tautomerism step is an irreversible phenomenon, the chance of the increment of amorphous content in this 3D porphyrin-based COF is much higher. As a result, there may be much less π···π stacking in this amorphous 3D framework, compared to the crystalline 2D porphyrin-containing COFs.

Hence, in order to enhance the chemical stability and crystallinity in 2D porphyrin COFs, we have decided to switch to a new strategy to protect the COF interior by introducing -OH functionalities adjacent to the Schiff base [-C=N] centers in COFs and thereby creating an intramolecular O–H···N=C hydrogen bond (Scheme 1). This hydrogen-bonding interaction helps to protect the basic imine nitrogen from hydrolysis in the presence of water and acid. This newly synthesized COF, DhaTph, can retain its crystallinity in 3 N HCl and deionized water for more than one week. We found that apart from its stability, this hydrogen bond in DhaTph enhances the crystallinity and porosity. To validate this result, we have synthesized the methoxy-substituted COF DmaTph in which this intramolecular hydrogen bond does not exist. DmaTph was found to have less crystallinity, chemical stability, and porosity compared to DhaTph.

Syntheses of DmaTph and DhaTph were done by the Schiff base reaction between 2,5-dimethoxyterephthalaldehyde (Dma) (15.5 mg, 0.08 mmol) or 2,5-dihydroxyterephthalaldehyde (Dha) (13.3 mg, 0.08 mmol) and 5,10,15,20-tetrakis(4-aminophenyl)-21*H*,23*H*-porphine (Tph) (27.0 mg, 0.04 mmol) in the presence of 6 M acetic acid (0.2 mL) using dichlorobenzene and ethanol (1:1) as the solvent combination (2 mL; Scheme 1). PXRD patterns of DhaTph show a highly intense peak at 3.4° (intensity around 70 000 cps; cps = counts

[*] S. Kandambeth, D. B. Shinde, M. K. Panda, Dr. R. Banerjee
Physical/Materials Chemistry Division
CSIR-National Chemical Laboratory
Dr. Homi Bhabha Road, Pune-411008 (India)
E-mail: r.banerjee@ncl.res.in
B. Lukose, Dr. T. Heine
Center for Functional Nanomaterials
School of Engineering and Science
Jacobs University Bremen, Bremen, 28759 (Germany)

[**] S.K. and D.B.S. acknowledge CSIR, New Delhi, India, for fellowships. R.B. acknowledges CSIR's five year plan (grant numbers CSC0122 and CSC0102) for funding. Financial assistance from the European Research Council (ERC grant numbers StG C3ENV and GA 256962) and BRNS (grant number 2011/37C/44/BRNS) is acknowledged. We acknowledge Dr. T. G. Ajithkumar for providing NMR and Dr. C. Ramesh for PXRD facilities.

Supporting information for this article is available on the WWW under http://dx.doi.org/10.1002/anie.201306775.

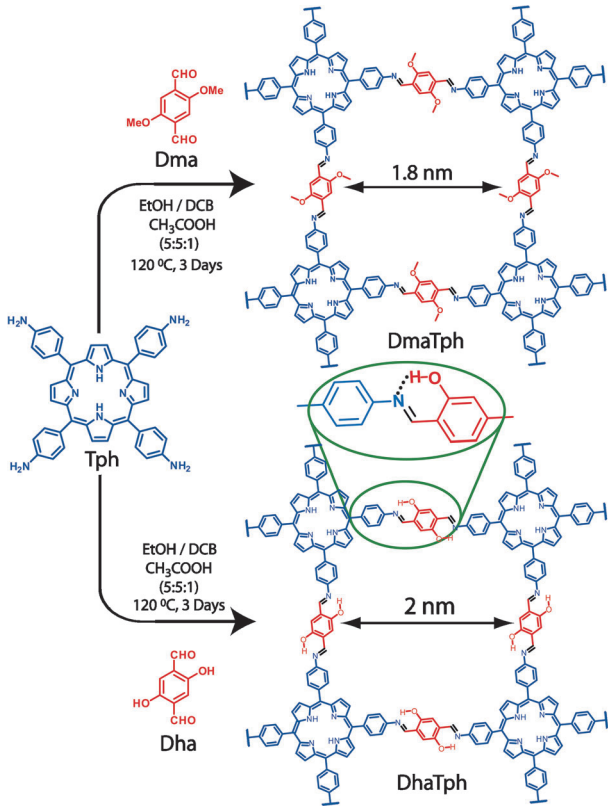

Scheme 1. Syntheses of DmaTph and DhaTph by the condensation of square planar Tph building unit (blue) and linear Dma/Dha building unit (red).

per second) which corresponds to the 100 plane reflections (Figure 1 a). PXRD patterns of DhaTph also show minor peaks at 6.9° and 20–23° 2θ which corresponds to the 200 and 001 facets. The π–π stacking distance between COF layers was calculated as 3.8–4.4 Å from the *d* spacing between the 001 plane. PXRD peaks for DmaTph were found to appear almost at the same position to that of DhaTph. Peaks at 3.4°, 6.8°, and 17–25° correspond to the 100, 200, and 001 facets, respectively. But the peak intensity of the 100 plane (around 3000 cps) has been considerably reduced compared to DhaTph (Figure 1 a). The reason behind this difference in crystallinity among these two COFs is the presence of O–H···N=C intramolecular hydrogen bonding in DhaTph, which holds all phenyl rings in one plane and keeps all imine bonds in the trans conformation (see section S14 in the Supporting Information). This intramolecular O–H···N=C hydrogen bond, along with the trans -C=N bond, reduces structural defects, and enhances structural rigidity in DhaTph, leading to an improved crystallinity. However, DmaTph does not contain such hydrogen bonding, as the porphyrin (Tph) units are connected by 2,5-dimethoxyterephthalaldehyde units where these -OH functionalities have been replaced by -OCH_3 groups. As a result, planarity and structural rigidity between the phenyl rings were lost in DmaTph (Figure 1 f). This loss in planarity between the phenyl rings decreases the stacking between the 2D layers and subsequently reduces the crystallinity in DmaTph (Figure 1 e). We crystallized the linker units of DhaTph and DmaTph in order to understand the effect of hydrogen bonding on the planarity of the structure (Figure 1 f and g). It is evident, from the single-crystal data, that intramolecular O–H···N=C hydrogen bonding [$D = 2.619(2)$ Å, $d = 1.895(2)$ Å, and $\theta = 146.6°$ (3)] exists in the linker unit of DhaTph and the structure is completely planar (Figure 1 g). However, the DmaTph linker unit is nonplanar as it does not contain this intramolecular O–H···N=C hydrogen bonding (Figure 1 f). In order to elucidate the structure of these COFs and to calculate the unit cell parameter, a possible 2D model was built using the self-consistent charge density functional tight-binding (SCC-DFTB) method.[10] The experimental PXRD pattern matches well with the simulated pattern of the eclipsed stacking model (Figure 1 b). Hence, we propose a structure close to the *P*4/m space group for DhaTph and DmaTph, after comparing the

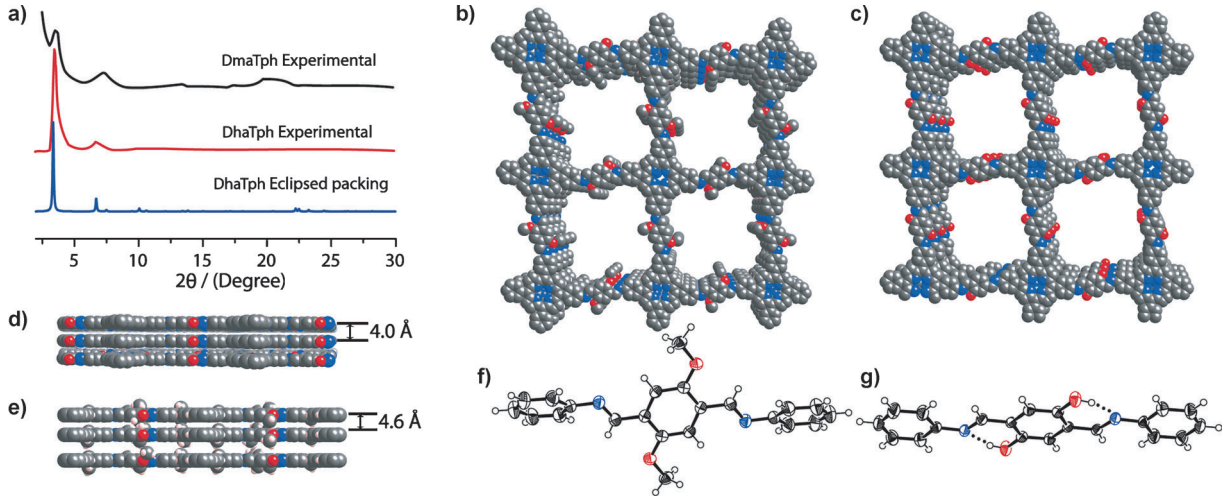

Figure 1. a) The experimental PXRD pattern of DhaTph (red) compared with simulated eclipsed (blue), PXRD pattern of DmaTph (black) indicates moderate crystallinity. b) Stacking diagram of DhaTph. c) Stacking diagram of DmaTph shows irregular layer stacking. d) Eclipsed stacking model of DhaTph. e) Eclipsed stacking model of DhaTph. f) ORTEP diagram of DmaTph linker unit shows structure is nonplanar. g) ORTEP diagram of DhaTph linker unit shows the presence of the intramolecular hydrogen bond; all atoms are in one plane.

experimental PXRD pattern with the simulated one (Figure 1a). The unit cell values of DhaTph and DmaTph were calculated to be ($a=b=25.6$ Å, $c=4$ Å) using the Pawley refinement (see section S4).

The total consumption of starting materials, after the COF formation reaction, was indicated by the disappearance of the -N–H stretching bands (3100–3400 cm^{-1}) of Tph and the C=O stretching bands of Dma (1670 cm^{-1}) and Dha (1660 cm^{-1}) in the FTIR spectrum (Figure 2a). The FTIR spectrum of

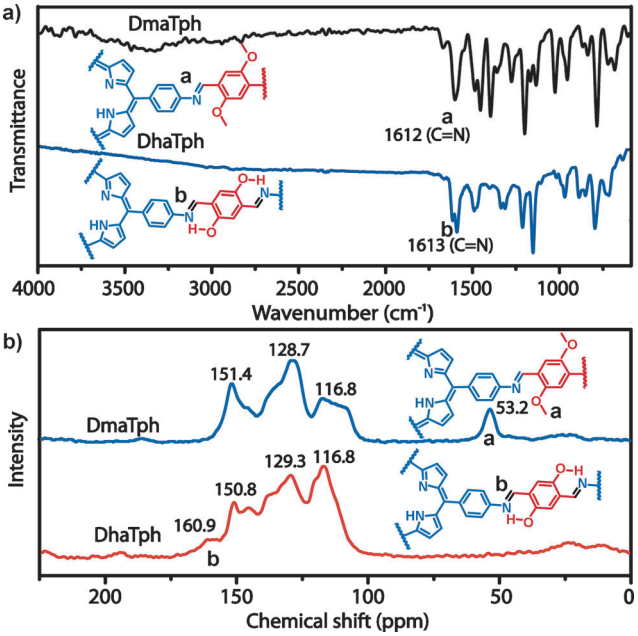

Figure 2. a) Comparison of FTIR spectra of DmaTph (black) and DhaTph (red). b) Comparison of solid-state ^{13}C NMR spectra of DmaTph (blue) and DhaTph (red).

DhaTph shows characteristic -C=N stretching bands at 1613 cm^{-1}, which appear almost at the same position as in the linker unit of DhaTph (1611 cm^{-1}; Figure S6) and COF-366 (1620 cm^{-1}).[9] Hence, we can conclude that DhaTph exists in the enol-imine form. For DmaTph, the -C=N stretching band appears around 1612 cm^{-1}, which is close to 1613 cm^{-1}, the -C=N stretching value of the DmaTph linker unit. The ^{13}C CP-MAS solid-state NMR spectrum of DhaTph confirms the formation of the imine bond by showing the characteristic signal at δ 160.9, which corresponds to the chemical shift of the -C=N carbon. These values are close to the chemical shift of -C=N (δ 161.8) in the linker unit of DhaTph (Figure S14). To provide supporting evidence for the existence of the enol-imine form, we have crystallized the compound 2,5-bis((*E*)-(phenylimino)methyl)-benzene-1,4-diol) and (2,5-dimethoxy-1,4-phenylene)bis(*N*-phenylmethanimine) (linker unit present in DhaTph and DmaTph) by the Schiff base reaction between Dha/Dma and aniline (section S2). From the single-crystal data, it was evident that the compound exists only in the enol-imine form, which was reflected in the structure of DhaTph and DmaTph (Figure 1 f and g). The desired enol-to-keto tautomerism was not observed in DhaTph because of the absence of polarized molecules in the system.[11] The ^{13}C cross-polarized magic angle spinning (CP-MAS) solid-state NMR spectrum of DmaTph is almost similar to that of DhaTph but contains an extra signal in the up-field region around δ 53.2, which corresponds to the -OCH_3 group (Figure 2b). TEM images revealed that DhaTph is composed of well-defined, square-shaped particles that have a uniform size of around 50 nm (Figure S27). DmaTph particles were much more elongated in shape, forming rectangular or belt-shaped structures (width up to 50 nm and length more than 200 nm; Figure S28).

Thermogravimetric analysis (TGA) was done on activated DhaTph and DmaTph to determine the thermal stability and to confirm the absence of guest molecules inside the pores (section S9). Both COFs show thermal stability up to 300 °C. A gradual weight loss of 50 % for DhaTph and 40 % for DmaTph was observed after 300 °C because of the decomposition of the framework. Permanent porosity of DhaTph and DmaTph were evaluated by the N_2 adsorption isotherm. Both DhaTph and DmaTph show a reversible type IV adsorption isotherm with H3 hysteresis. A sharp rise occurs in the initial state of the N_2 adsorption isotherms (0–0.1 bar) because of the filling of small pores, followed by gradual uptake over the remaining pressure range (Figures S15 and S18). The steep increase of N_2 uptake shown at high relative pressure ($P/P_0>0.8$)) was due to the condensation in the interparticle voids. The surface area of the COFs reported herein has been calculated with the application of the Brunauer–Emmett–Teller (BET) model, and found to be 1305 $m^2 g^{-1}$ for DhaTph and 431 $m^2 g^{-1}$ for the methyl-substituted DmaTph (Figures S14 and S17). The improved surface area of the DhaTph compared to DmaTph and COF-366 (735 $m^2 g^{-1}$)[9] can be considered as a result of the improved crystallinity of this material because of the strong intramolecular O–H···N=C hydrogen bond. The value is also comparable with CuP-$TFPh_{50}$, in which a higher crystallinity and surface area value were obtained as a result of a self-complementary π–π interaction.[12] The lower surface area value for the DmaTph was a result of its moderate crystallinity, together with the incorporation of bulky methyl group towards the pore walls. Langmuir surface areas calculated for both the COFs also show a similar trend: DhaTph has a higher Langmuir surface area (1900 $m^2 g^{-1}$) than DmaTph (740 $m^2 g^{-1}$). The NLDFT model was used to study the pore size distributions. The pore size distribution plot of DhaTph shows a peak maxima at 2.0 nm and a pore volume of 0.809 $cm^3 g^{-1}$ which is close to the theoretically calculated pore width of 2.1 nm. The peak maxima for DmaTph appear at a lower value of around 1.5 nm (Figures S17 and S20). The H_2 uptake of DhaTph and DmaTph was found to be 171 $cm^3 g^{-1}$ and 78 $cm^3 g^{-1}$, respectively, at 77 K and a pressure of 1 atm. The CO_2 uptake of DhaTph was measured as 65 $cm^3 g^{-1}$, while DmaTph showed a lower CO_2 uptake of 37 $cm^3 g^{-1}$ at 273 K and a pressure of 1 bar (Figure S20).

Even though the desired enol–keto tautomerism did not happen in DhaTph, the compound remained stable while directly submerged in water for more than seven days. This observation encouraged us to make a detailed investigation of the stability of DhaTph and DmaTph in water, acid, and base.

To investigate the stability, 50 mg of each COF was directly submerged in 10 mL water and kept boiling for a period of seven days. After this time period, COF powders were filtered, dried, and the retention of crystallinity was tested by PXRD. It was observed that the relative peak intensity and peak position of DhaTph remained identical after this prolonged water treatment (Figure 3a). The change in

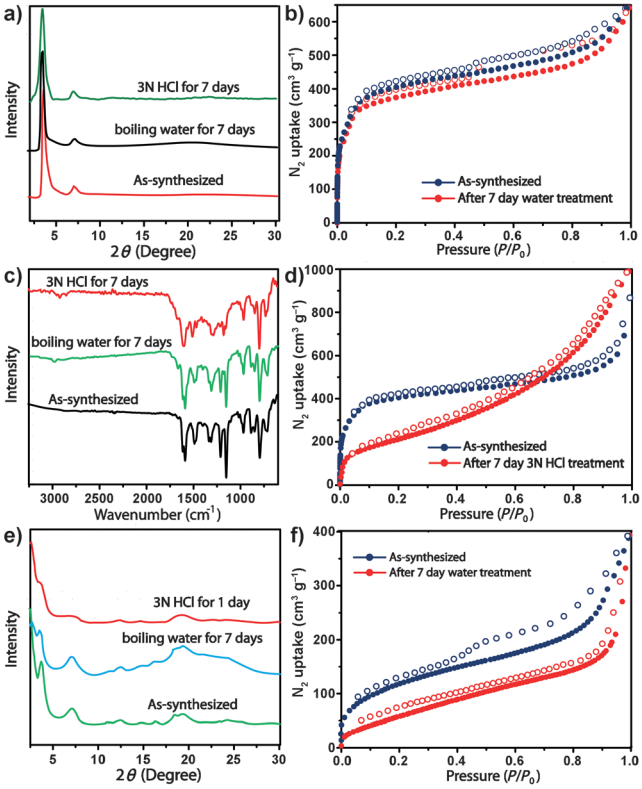

Figure 3. a) PXRD pattern showing the stability of DhaTph. b) N_2 adsorption isotherms at 77 K of DhaTph before (blue) and after treatment with boiling water for 7 days (red). c) FTIR spectra showing the stability of DhaTph. d) N_2 adsorption isotherms at 77 K of DhaTph before (blue) and after treatment with 3 N HCl acid for 7 days (red). e) PXRD pattern of DmaTph showing the loss of crystallinity after 1 day. f) N_2 adsorption isotherms at 77 K of DmaTph before (blue) and after treatment with boiling water for 7 days (red).

porosity (1305 $m^2 g^{-1}$ before and 1252 $m^2 g^{-1}$ after water treatment) of the material was also negligible, as indicated by the N_2 adsorption studies (Figure 3b). This enhancement of water stability of the DhaTph is extremely important, because similar analogous COFs, such as COF-366[7] and CuP-Ph COF[11], need anhydrous organic solvents for washing and purification. The intramolecular hydrogen-bonding interaction is the key factor for this enhanced hydrolytic stability of DhaTph. A similar kind of stability test was conducted on the methoxy analog DmaTph, in which no intramolecular hydrogen-bonding interaction exists. As anticipated, the crystallinity of DmaTph gets significantly lowered within 24 h, as indicated by the reduced peak intensity in the PXRD pattern (Figure 3e). N_2 adsorption isotherms (Figure 3f) were collected for the water treated DmaTph samples, and found to be decreased to almost 1/4th relative to the synthesized sample [229 $m^2 g^{-1}$]. To determine the stability in acid, 50 mg of DhaTph and DmaTph was submerged in 3 N HCl for 7 days. An immediate green coloration to the solution was observed initially in both cases. After the acid treatment, COF powders were filtered, washed with adequate amounts of water and ethanol, and finally dried at 90 °C. It was found that DhaTph suffers a weight loss of about 5 % after the acid treatment, but for DmaTph, almost all the material leached out. It was amazing to see that DhaTph retained its exact crystallinity after this long acid treatment, but the SEM image indicated a minor change in the morphology (Figure 3a). This experiment confirms that our strategy of protecting the -C=N centers in DhaTph by intramolecular hydrogen bonds was correct, as DhaTph shows high water and acid [3 N HCl for 7 days] stability. The porosity and surface area measurements of the acid-treated DhaTph shows a significant change (1305 $m^2 g^{-1}$ before and 570 $m^2 g^{-1}$ after treatment). This decrease in the surface area could be probably due to the protonation of the inner porphyrin core by HCl (section S15). PXRD was recorded for the recovered sample of DmaTph after the acid treatment after 24 h (Figure 3e). It was seen that most of the PXRD peaks disappeared after the treatment with acid (Figure 3e). We were unable to perform the N_2 adsorption studies since the recovered samples were very limited. For the base stability test, the same protocol was followed using 3 N NaOH. But this time, almost 70 % weight loss occurred to DhaTph and the solution color changed to deep red, which indicates the base instability of the sample. The high stability of DhaTph towards acid and water is a result of intramolecular O–H···N=C hydrogen-bonding interactions.[13] The labile imine bond nitrogen is protected from hydrolysis because of the strong hydrogen-bonding interaction. The preference for hydrogen-bond formation between the target acceptor and a phenolic -OH group is -C=N >-NO_2, -C=O >-P=O, and -F >-CF_3.[14] Thus, the O–H···C=N hydrogen-bonding interaction is found to be the strongest, which helps to improve the chemical stability and structural rigidity of the materials. In DmaTph, no such hydrogen bond exists, which results in ready decomposition of DmaTph in the lower pH region, just like other Schiff base polymers.[15]

We would like to conclude this report by mentioning that we were able to introduce a new strategy of intramolecular hydrogen bonding as an extra tool in COFs to improve the crystallinity, porosity, and chemical stability of the material. We have validated our results by removing this hydrogen bond using the methoxy analog that showed lower stability and crystallinity. We expect this method to broaden the scope of synthesizing highly crystalline and stable 2D COFs, which can perform better than its non-hydroxy analogs for gas storage and organic photovoltaic applications.

Received: August 2, 2013
Published online: October 14, 2013

Keywords: covalent organic frameworks · hydrogen bonds · mesoporous materials · porphyrinoids · tautomerism

[1] a) A. P. Cote, A. I. Benin, N. W. Ockwig, M. O'Keeffe, A. J. Matzger, O. M. Yaghi, *Science* **2005**, *310*, 1166; b) X. Feng, L. Chen, Y. P. Dong, D. Jiang, *Chem. Commun.* **2011**, *47*, 1979; c) E. L. Spitler, W. R. Dichtel, *Nat. Chem.* **2010**, *2*, 672; d) J. W. Colson, W. R. Dichtel, *Nat. Chem.* **2013**, *5*, 453.

[2] a) M. O'Keeffe, B. G. Hyde, *Crystal Structures I. Patterns and Symmetry*, Mineralogical Society of America, Washington, DC, **1996**; b) N. W. Ockwig, O. Delgado-Friedrichs, M. O'Keeffe, O. M. Yaghi, *Acc. Chem. Res.* **2005**, *38*, 176.

[3] a) H. Li, M. Eddaoudi, M. O'Keeffe, O. M. Yaghi, *Nature* **1999**, *402*, 276; b) C. Janiak, *Dalton Trans.* **2003**, 2781.

[4] a) X. Feng, X. Ding, D. Jiang, *Chem. Soc. Rev.* **2012**, *41*, 6010; b) S. Y. Ding, W. Wang, *Chem. Soc. Rev.* **2013**, *42*, 548.

[5] a) X. Ding, J. Guo, X. Feng, Y. Honsho, J. Guo, S. Seki, P. Maitarad, A. Saeki, S. Nagase, D. Jiang, *Angew. Chem.* **2011**, *123*, 1325; *Angew. Chem. Int. Ed.* **2011**, *50*, 1289; b) M. Dogru, M. Handloser, F. Auras, T. Kunz, D. Medina, A. Hartschuh, P. Knochel, T. Bein, *Angew. Chem.* **2013**, *125*, 2992; *Angew. Chem. Int. Ed.* **2013**, *52*, 2920; c) S. Wan, J. Guo, J. Kim, H. Ihee, D. Jiang, *Angew. Chem.* **2008**, *120*, 8958; *Angew. Chem. Int. Ed.* **2008**, *47*, 8826; d) X. Feng, L. Liu, Y. Honsho, A. Saeki, S. Seki, S. Irle, Y. Dong, A. Nagai, D. Jiang, *Angew. Chem.* **2012**, *124*, 2672; *Angew. Chem. Int. Ed.* **2012**, *51*, 2618.

[6] a) T. Ben, H. Ren, S. Ma, D. Cao, J. Lan, X. Jing, W. Wang, J. Xu, F. Deng, J. M. Simmons, S. Qiu, G. Zhu, *Angew. Chem.* **2009**, *121*, 9621; *Angew. Chem. Int. Ed.* **2009**, *48*, 9457; b) P. Kuhn, M. Antonietti, A. Thomas, *Angew. Chem.* **2008**, *120*, 3499; *Angew. Chem. Int. Ed.* **2008**, *47*, 3450; c) A. Bhunia, V. Vasylyeva, C. Janiak, *Chem. Commun.* **2013**, *49*, 3961.

[7] a) L. M. Lanni, R. W. Tilford, M. Bharathy, J. J. Lavigne, *J. Am. Chem. Soc.* **2011**, *130*, 11872; b) Y. Du, K. Mao, P. Kamakoti, P. Ravikovitch, C. Paur, S. Cundy, Q. Li, D. Calabro, *Chem. Commun.* **2012**, *48*, 4606.

[8] S. Kandambeth, A. Mallick, B. Lukose, N. V. Mane, T. Heine, R. Banerjee, *J. Am. Chem. Soc.* **2012**, *134*, 19524.

[9] S. Wan, F. Gandara, A. Asano, H. Furukawa, A. Saeki, S. K. Dey, L. Liao, M. W. Ambrogio, Y. Y. Botros, X. Duan, S. Seki, J. F. Stoddart, O. M. Yaghi, *Chem. Mater.* **2011**, *23*, 4094.

[10] B. Lukose, A. Kuc, T. Heine, *Chem. Eur. J.* **2011**, *17*, 2388.

[11] B. M. Drašković, G. A. Bogdanović, M. A. Neelakantan, A. C. Chamayou, S. Thalamuthu, Y. S. Avadhut, J. S. Günne, S. Banerjee, C. Janiak, *Cryst. Growth Des.* **2010**, *10*, 1665.

[12] X. Chen, M. Addicoat, S. Irle, A. Nagai, D. Jiang, *J. Am. Chem. Soc.* **2013**, *135*, 546.

[13] a) A. C. Dash, R. K. Nanda, *J. Am. Chem. Soc.* **1969**, *91*, 6944; b) P. Di Bernardo, P. L. Zanonato, S. Tamburini, P. Tomasinb, P. A. Vigatob, *Dalton Trans.* **2006**, 4711.

[14] a) G. R. Desiraju, T. Steiner, *The Weak Hydrogen Bond in Structural Chemistry and Biology*, Oxford University Press, Oxford, **1999**; b) A. Kovács, A. Szabó, I. Hargittai, *Acc. Chem. Res.* **2002**, *35*, 887.

[15] Y. Xin, J. Yuan, *Polym. Chem.* **2012**, *3*, 3045.

